Proceedings of the ASME 2019 38th International Conference on Ocean, Offshore and Arctic Engineering
OMAE2019
June 9-14, 2019, Glasgow, Scotland

OMAE2019-96098

DEVELOPMENT OF 3-DIMENSIONAL FULLY NONLINEAR POTENTIAL FLOW WAVE TANK IN FRAMEWORK OF OPENFOAM

Zaibin Lin[1], Ling Qian, Wei Bai, Zhihua Ma, Hao Chen, Jian-Guo Zhou
Manchester Metropolitan University, John Dalton Building, Manchester Campus
Manchester, the United Kingdom

ABSTRACT

A 3-Dimensional numerical wave tank based on the fully nonlinear potential flow theory has been developed in OpenFOAM, where the Laplace equation of velocity potential is discretized by Finite Volume Method. The water surface is tracked by the semi-Eulerian-Lagrangian method, where water particles on the free surface are allowed to move vertically only. The incident wave is generated by specifying velocity profiles at inlet boundary with a ramp function at the beginning of simulation to prevent initial transient disturbance. Additionally, an artificial damping zone is located at the end of wave tank to sufficiently absorb the outgoing waves before reaching downstream boundary. A five-point smoothing technique is applied at the free surface to eliminate the saw-tooth instability. The proposed wave model is validated against theoretical results and experimental data. The developed solver could be coupled with multiphase Navier-Stokes solvers in OpenFOAM in the future to establish an integrated versatile numerical wave tank for studying efficiently wave structure interaction problems.

Keywords: OpenFOAM, Finite Volume Method, Fully Nonlinear Potential Flow, Numerical Wave Tank.

INTRODUCTION

Simulation of water waves propagating in shallow water and deep water zones in a computationally robust and cost-efficient manner is still a big challenge for both nearshore and offshore engineering applications. When dealing with fully nonlinear wave-structure interaction for industrial problems, it usually requires an efficient and accurate numerical model. Driven by this demand, various numerical models, based on Navier-Stokes (N-S) equations, Boussinesq equations, and Fully Nonlinear Potential Flow Theory (FNPFT), have been proposed to address the engineering problems of nonlinear wave interaction with offshore/coastal structures. Recently, two open-access numerical wave generation and absorption solvers, i.e., waves2Foam [1] and IHFOAM [2, 3] based on incompressible two-phase N-S equations, have been proposed. These solvers have been extensively used to investigate a wide range of offshore and coastal engineering problems [4-7]. Due to the application of Volume of Fluid (VoF) method [8], these solvers can handle violent wave structure interactions involving wave breaking and air entrainment, where the potential flow model fails substantially. Unfortunately, the numerical wave tanks based on N-S equations are extremely time-consuming especially for very large scale problems. For non-breaking wave propagation and transformation, as an alternative, FNPFT model can provide accurate numerical results much more efficiently, and this is highly desirable in engineering applications [9-12].

Successful implementation of the FNPFT model can be found in the literature, where researchers used Finite Difference Method (FDM) [13, 14], Finite Element Method (FEM) [15, 16], Finite Volume Method (FVM), Higher Order Boundary Element Method (HOBEM) [17, 18] to solve the Laplace equation. . However, the investigation of the FNPFT model in a finite volume based framework is very limited. To the best knowledge of the authors, the only attempt dealing with the FNPFT model in a finite volume framework was reported by Mehmood et al. [19], where they presented a few preliminary results of 2D linear wave propagation in an empty wave tank. Whether the developed finite volume based numerical model can deal with nonlinear waves or more complex 3-D wave structure interaction problems, which is a must for real applications, has not been demonstrated by the authors.

The objective of this study is to develop an efficient 3-D FNPFT model based numerical wave tank using the finite volume solution methodology. We use the open source CFD library OpenFOAM as the framework to implement the 3-D

[1] Contact author: zaibin.lin@gmail.com

FNPFT model. The remainder of the paper is organised as follows. In Section 1.1, the mathematical formulations and numerical implementation for 3-D FNPFT are described in detail, followed by Section 1.2, which presents the numerical results and corresponding discussions. Lastly, the conclusions are drawn in Section 1.3.

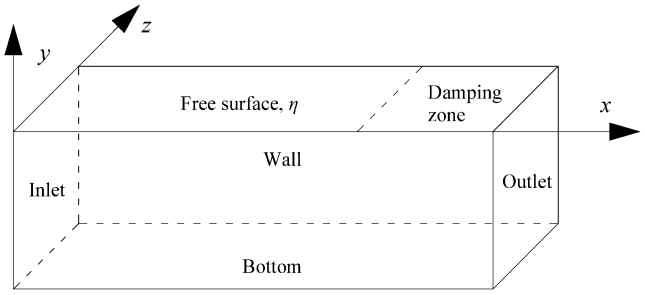

FIGURE 1: SKETCH OF NUMERICAL DOMAIN.

1.1 Mathematical formulations

Based upon the assumption of the irrotational flow and incompressible inviscid fluid, Laplace equation of velocity potential is considered here. A 3-D Cartesian coordinate system is used in the model, where the origin is located at the still water level and the *y*-axis is pointing vertically upwards in Fig. 1. The governing equations is described as:

$$\nabla^2\phi = 0 \tag{1}$$

where ϕ is velocity potential and ∇ is gradient operator. To solve free surface problems of water wave, both kinematic and dynamic boundary conditions in the following need to be specified at the free surface of numerical domain:

$$\frac{\partial\eta}{\partial t} = \frac{\partial\phi}{\partial y} - \frac{\partial\phi}{\partial x}\frac{\partial\eta}{\partial x} - \frac{\partial\phi}{\partial z}\frac{\partial\eta}{\partial z} \tag{2}$$

$$\frac{\partial\phi}{\partial t} = -g\eta - \frac{1}{2}\nabla\phi\cdot\nabla\phi \tag{3}$$

where η is free surface elevation, g= 9.81m/s^2 is gravitational acceleration, and t is time. Eqn. (2) can be formulated into Eqn. (4) by considering water particle velocity at the free surface [20]. Due to the mesh only moving vertically with the free surface and considering a semi-Eulerian-Lagrangian method, Eqn. (3) can be modified into Eqn. (5) with $\frac{\delta(\,)}{\delta t} = \frac{\partial(\,)}{\partial t} + \boldsymbol{U_m}\cdot\nabla(\,)$ and $\boldsymbol{U_m}$= (0, 0, $\frac{\partial\eta}{\partial t}$). For this modification, readers are referred to [21, 22] for details.

$$\frac{\partial\eta}{\partial t} = \frac{\boldsymbol{U}_\eta\cdot\boldsymbol{n}}{n_y} \tag{4}$$

$$\frac{\delta\phi}{\delta t} = -g\eta - \frac{1}{2}\nabla\phi\cdot\nabla\phi + \frac{\partial\eta}{\partial t}\frac{\partial\phi}{\partial y} \tag{5}$$

where $\boldsymbol{U}_\eta$ is the fluid particle velocity at free surface, $\boldsymbol{n}$ is the unit normal vector of free surface pointing outwards from the domain, and n_y is the vertical component of the unit normal vector $\boldsymbol{n}$. A sketch of numerical domain is presented in Fig. 1. In order to avoid the reflection wave, a wave damping zone is located at the end of numerical wave flume. In this zone, two additional terms should be added to both kinematic and dynamic boundary conditions, then in the damping zone Eqns. (4) and (5) become：

$$\frac{\partial\eta}{\partial t} = \frac{\boldsymbol{U}_\eta\cdot\boldsymbol{n}}{n_y} - v(x)(\eta-\eta_s) \tag{6}$$

$$\frac{\delta\phi}{\delta t} = -g\eta - \frac{1}{2}\nabla\phi\cdot\nabla\phi + \frac{\partial\eta}{\partial t}\frac{\partial\phi}{\partial y} - v(x)\phi \tag{7}$$

where $v(x) = \begin{cases}\omega\left(\frac{x-x_0}{\beta\lambda}\right)^2, & x > x_0\\ 0, & x < x_0\end{cases}$, in which x_0 is the start point of wave damping zone, β is the damping coefficient that equals to damping zone length, λ is incoming wave length, and ω is incoming wave frequency. Adding these two damping terms in both kinematic and dynamic boundary conditions will efficiently reduce the wave reflection from the end of wave flume.

When progressive wave is generated, the inlet in Fig. 1 is expressed as:

$$\frac{\partial\phi}{\partial x} = \boldsymbol{U}_x \tag{8}$$

where $\boldsymbol{U}_x$ is the analytical velocity component in the *x* direction of target wave. When the proposed 3-D FNPFT model is used to investigate sloshing phenomenon in a tank, the inlet and outlet are specified as impermeable boundaries as follow, which are also used at lateral walls and bottom of numerical domain:

$$\frac{\partial\phi}{\partial\boldsymbol{n}} = 0 \tag{9}$$

The mesh at the free surface in Fig. 1 deforms based on the kinematic boundary conditions in Eqns. (4) and (6) and the remaining mesh inside the domain is updated accordingly, which will be used to solve Eqn. (1) in the next time step. Then, velocity field of whole domain will be obtained by solving $\mathbf{U} = \nabla\phi$ and adopted to update free surface elevation η and mesh point deformation at free surface, which are smoothed by five-points smoothing technique. This loop is the simulation process of this 3-D Fully Nonlinear Potential Flow Theory model in OpenFOAM.

1.2 Results and discussion

In this section, the newly developed FNPFT model in OpenFOAM will be used to investigate 3-D sloshing, wave generation, and two wave shoaling cases, respectively. First, the 3-D sloshing case is introduced and compared with analytical results and numerical results available in the literature. By introducing wave generation boundary condition (see Eqn. (*8*)),

the progressive wave is generated in the 3-D numerical wave tank, and validated against analytical results. Afterwards, a representative benchmark shoaling case along a submerged bar is numerically simulated using proposed FNPFT model with comparison to experimental data. Lastly, a 3-D numerical wave propagation in a wave tank, where a semi-circular slope is located in the middle, is presented to demonstrate the capacity of present model in simulating 3-D wave propagation and transformation.

The first validation case to be presented is a classical 3-D wave sloshing in a container with the effect of gravity. The container in Fig. 2 has a length 1m and a width 0.2 m, as well as the initial slope of 0.02 and still water depth 0.2 m. When simulation starts, the gravity and the wave level difference between two ends of the container can drive the fluid to move periodically in this 3-D container.

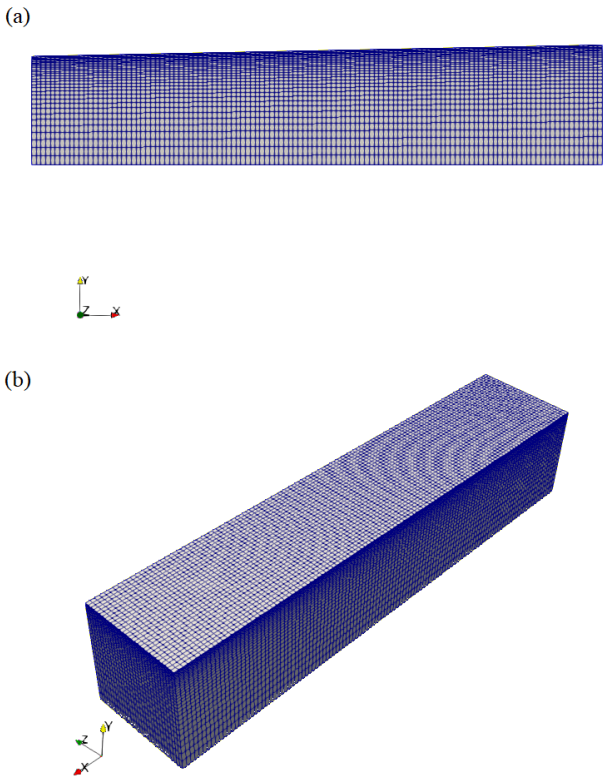

FIGURE 2: SKETCH OF A 3-D WAVE SLOSHING CONTAINER.

Simulated results of wave sloshing using present FNPFT model are compared with analytical solutions according to linear wave theory (see [23] for details). In OpenFOAM, two mesh layouts are used in the cases, including 120×30×20 cells and 60×12×20 cells in x, y, and z direction, respectively, with vertical mesh refinement near free surface. The comparison between numerical and analytical results for wave sloshing are presented in Fig. 3, from which it can been seen that the numerical results based on FNPFT in OpenFOAM present better agreement with analytical results. Moreover, the case with refined mesh provides more accurate results compared to the coarser mesh case and the numerical results in [24].

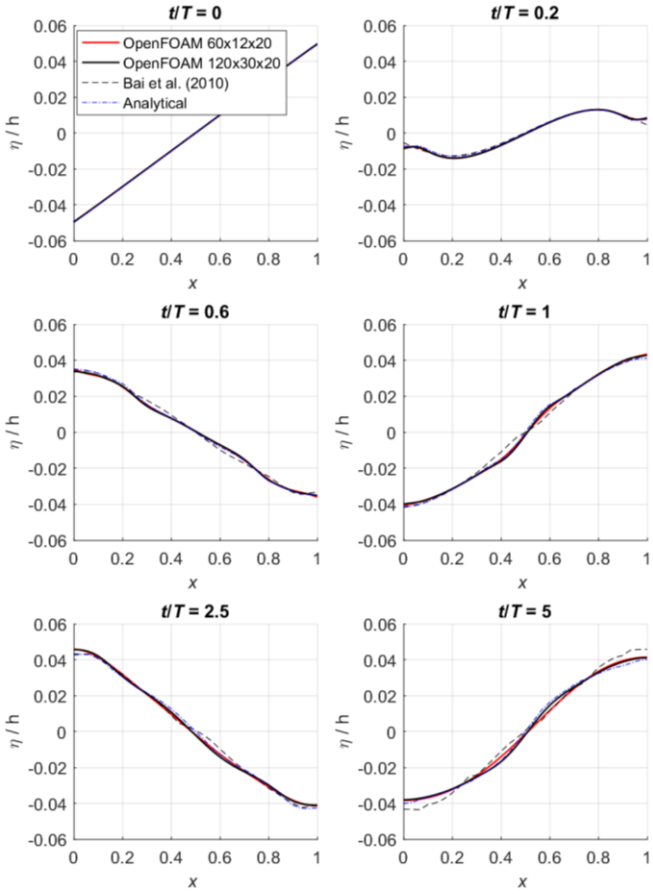

FIGURE 3: COMPARISON OF NUMERICAL AND ANALYTICAL FREE SURFACE ELEVATION OF WAVE SLOSHING

To investigate the capacity of present FNPFT model in wave generation, a 3-D numerical wave tank was established as shown in Fig. 1 with a wave generation boundary condition at the inlet (see Eqn. (*8*)) and a wave damping zone near the outlet (see Eqns. 6 and 7). A wave with wave amplitude A of 0.025m, wave period of 1.0s and water depth d of 0.28m, was selected and validated against analytical solutions. A 3-D numerical wave tank with length of 11 m, width of 1 m, and depth of 0.28 m was set-up for validation. In this case, the length of wave damping zone is set twice wave length, hence β in Eqns. 6 and 7 equals 2. The mesh size for this numerical wave tank is 400×30×20 in x, y, and z direction, respectively, and the mesh is vertically refined in the vicinity of free surface.

In this case, the wave has been simulated for 30 wave periods to examine the stability of the proposed FNPFT model in wave generation. Two snapshots of this 3-D numerical wave tank are presented in Fig. 4, where the mesh refinement and vertical mesh deformation in the direction are clearly indicated. During wave propagation, the mesh moves up and down

vertically according to kinematic boundary condition in Eqns. (4) and (6).

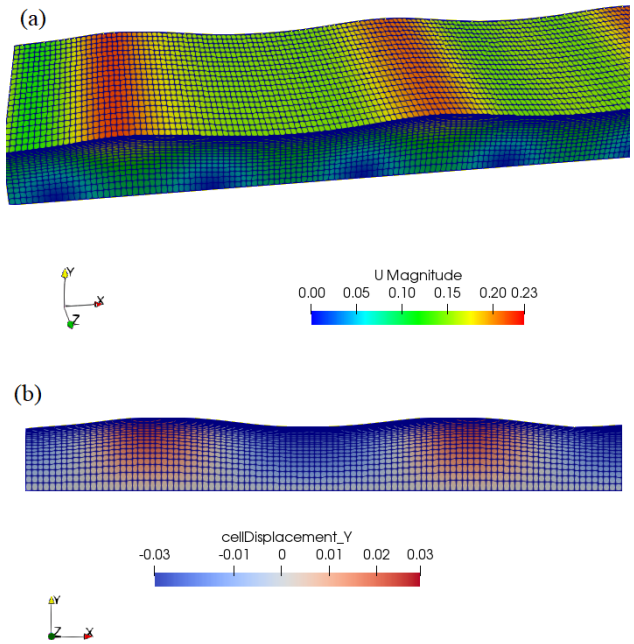

FIGURE 4: SNAPSHOTS OF VELOCITY MAGINITUDE FIELD AND MESH MOVEMENTS NEAR THE INLET

In Fig. 5, the time histories of numerical progressive wave at three wave gauges (x = 0.5 m, 5.5 m, and 8 m) is presented together with analytical results of second-order Stokes wave theory. The error is defined as the normalization of the difference between numerical and analytical results by target wave amplitude. It can be obviously seen at the Wave Gauge 1 (WG1) in Fig. 5 that the wave generated from inlet boundary has very good agreement with analytical solution, while slight discrepancy can also be noted due to minor wave reflection from the outlet. In the centre of wave tank, where WG2 is located, similar difference between numerical and analytical results is also shown due to the effect of wave reflection. This phenomenon is more significant at WG3 due to its location closer to the wave damping zone. Therefore, after approximately 16 wave periods, the wave phase becomes slightly different from analytical solution, while the wave amplitude is still acceptable. In overall, the good agreement between numerical and analytical results in Fig. 5 indicates that the present FNPFT model is able to numerically reproduce progressive waves in the 3-D wave tank.

In order to further demonstrate the ability of present FNPFT model in predicting wave transformation, a progressive wave over a submerged bar is presented, which is the so-called wave shoaling case. The set-up of 3-D numerical wave tank for wave shoaling can be found in Fig. 6, where the tank length is 35 m, tank width is 1 m, and the water depth varies along the wave tank. Four wave gauges (WGs), which are located at x = 2.0 m, 12.5 m, 14.5 m. and 17.3 m, respectively, are selected in the wave tank to measure the incident wave and shoaling progress along the submerged bar. In this case, the progressive wave is generated from the inlet boundary with wave amplitude of 0.01m, wave period of 2.02 s, and water depth of 0.4 m. The mesh size for the 3-D numerical domain is 700×30×20 in x, y, and z direction, respectively. The mesh refined in the proximity of free surface and in the region with submerged bar in x direction in order to capture shorter waves after shoaling above the submerged bar.

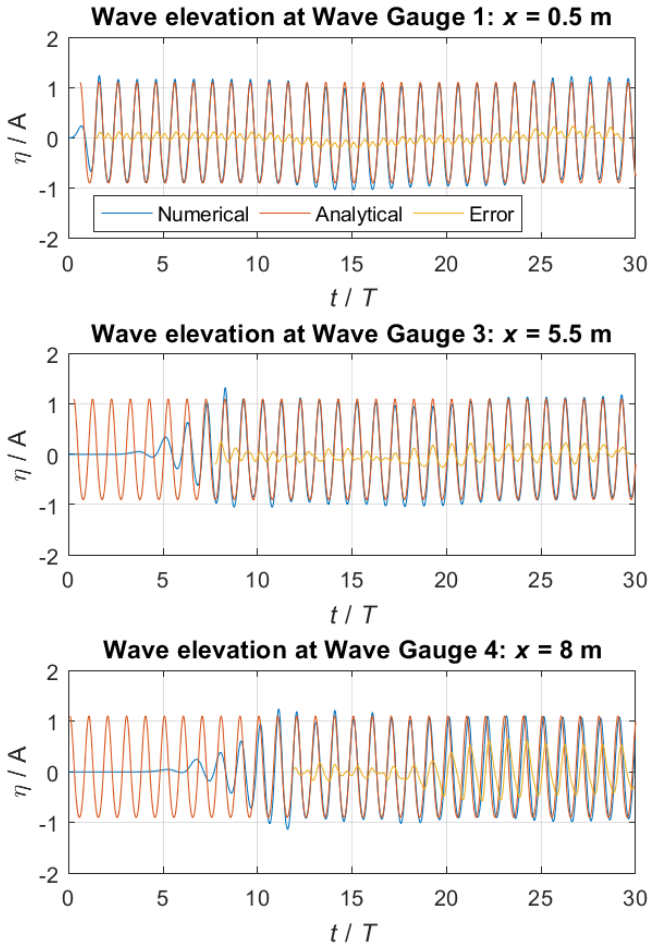

FIGURE 5: COMPARISON OF NUMERICAL AND ANALYTICAL WAVE PROFILES OF A PROGRESSIVE WAVE AT VARIOUS WAVE GAUGES

In Fig. 7, the time histories of free surface elevation at four wave gauges are presented and compared with experimental data from [25]. At WG1, the incident wave agrees very well with the experimental result, while a slight discrepancy can be found at WG4 (x = 17.3 m). But overall good agreement is clearly seen from the two remaining wave gauges. Therefore, it can be concluded that the wave shoaling has been accurately predicted using this newly developed 3-D FNPFT model in OpenFOAM.

The last numerical simulation shown in Fig. 8 is a wave shoaling case over a semi-circular slope located in the middle of the wave tank. The still water depth is defined as follows: (1) the water depth at left flat bottom is 0.4572 m with $0 \le x \le 10.67$-G(z),

where G(z) =$\sqrt{z(6.096-z)}$; (2) the water depth at semi-circular slope is described as $0.4572+\frac{1}{25}(10.67-\mathrm{G}(z)-x)$ at $10.67-\mathrm{G}(z)<x<18.29-\mathrm{G}(z)$; (3) the water depth at right flat bottom is 0.1524 m with $18.29-\mathrm{G}(z)\leq x\leq 35.0$. In this case, a wave with A = 0.0075 m and T = 2 s is generated at the inlet at the deeper region and propagates to the shallower region through a semi-circular slope. It is then absorbed by a damping zone located at the right end of wave tank. During this process, a focusing region may be produced over the submerged semi-circular slope.

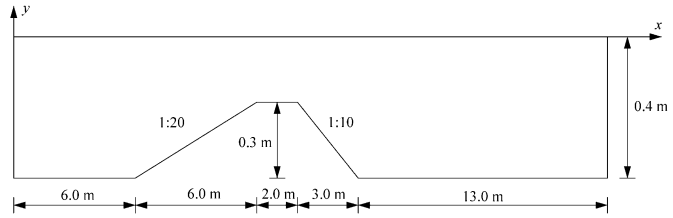

FIGURE 6: SKETCH OF NUMERICAL WAVE TANK FOR THE SHOALING TEST CASE

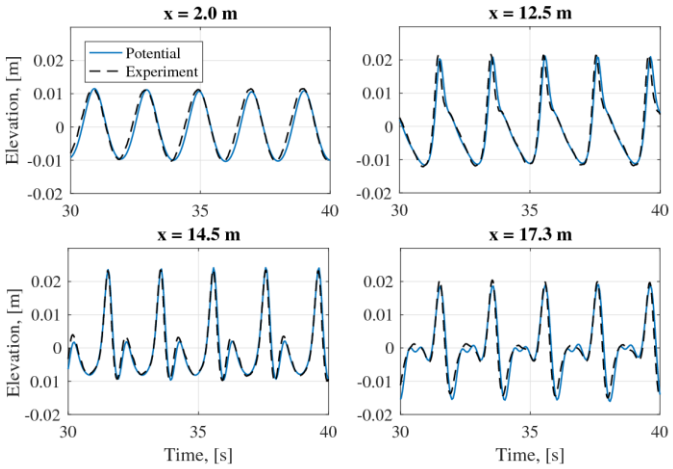

FIGURE 7: COMPARISON OF NUMERICAL RESULTS AND EXPERIMENTAL DATA AT FOUR WAVE GAUGES

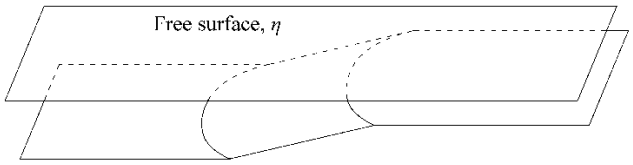

FIGURE 8: SKETCH OF A WAVE PROPAGATION OVER A SUBMERGED SEMI-CIRCULAR SLOPE (NOT IN SCALE)

A 2-D behaviour wave is generated from the inlet at left side of wave tank shown in Fig.9 (a), and propagates over the bottom topography. Due to the existence of a submerged semi-circular slope, the wave builds up 3-D effects in the focusing zone. Then it the keeps propagating over the shallower region before being absorbed by the damping zone. In the focusing zone, the free surface elevation has been significantly amplified with strongly 3-D effects compared to the wave amplitude generated at the inlet. It can be demonstrated that the present FNPFT model is able to properly capture the 3-D effects of wave propagation and transformation in a wave tank.

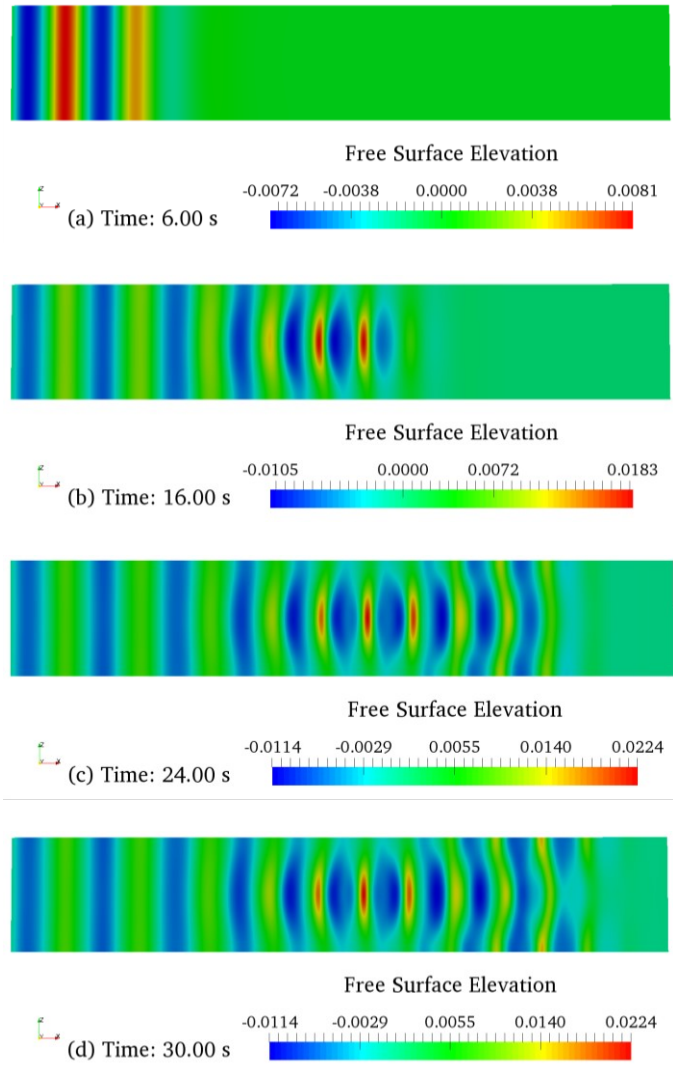

FIGURE 9: THE CONTOUR PLOTS OF FREE SURFACE ELEVATION AT DIFFERENT TIME

1.3 Conclusion

This paper presented a study on the development and validation of a 3-D FNPFT model in OpenFOAM. Based on the results from the validation test cases, it can be concluded that this newly developed FNPFT model in OpenFOAM is able to accurately capture the flow details of non-breaking free surface problems, including wave sloshing, wave propagation and transformation, wave shoaling over a submerged object. This

proposed FNPFT model is currently being integrated with Navier-Stokes multiphase flow solvers [26, 27] in OpenFOAM to construct an efficient hybrid numerical wave tank model for studying wave structure interaction problems. Compared to other hybrid free surface solvers using different numerical methods, the current approach is advantageous as both the FNPFT model and the Navier-Stokes solver are based on the finite volume method and in the same framework of OpenFOAM, which has clear implications for better solver compatibility and parallel efficiency.

ACKNOWLEDGEMENTS

We would like to acknowledge the financial support from the EPSRC (UK) for the Zonal CFD Project (EP/N008839/) and internal funds of Manchester Metropolitan University.

REFERENCES

[1] Jacobsen, N. G., Fuhrman, D. R., and Fredsøe, J., "A wave generation toolbox for the open-source CFD library: OpenFoam®," *International Journal for Numerical Methods in Fluids*, 70(9), 2012, pp. 1073-1088.

[2] Higuera, P., Lara, J. L., and Losada, I. J., "Realistic wave generation and active wave absorption for Navier–Stokes models: Application to OpenFOAM®," *Coastal Engineering*, 71, 2013, pp. 102-118.

[3] Higuera, P., Losada, I. J., and Lara, J. L., "Three-dimensional numerical wave generation with moving boundaries," *Coastal Engineering*, 101, 2015, pp. 35-47.

[4] Lin, Z., Pokrajac, D., Guo, Y., Jeng, D.-S., Tang, T., Rey, N., Zheng, J., and Zhang, J., "Investigation of nonlinear wave-induced seabed response around mono-pile foundation," *Coastal Engineering*, 121, 2017, pp. 197-211.

[5] Chen, H., and Christensen, E. D., "Investigations on the porous resistance coefficients for fishing net structures," *Journal of Fluids and Structures*, 65, 2016, pp. 76-107.

[6] Chen, H., and Christensen, E. D., "Development of a numerical model for fluid-structure interaction analysis of flow through and around an aquaculture net cage," *Ocean Engineering*, 142, 2017, pp. 597-615.

[7] Chen, H., and Christensen, E. D., "Simulating the hydrodynamic response of a floating net system in current and waves," *Journal of Fluids and Structures*, 79, 2018, pp. 50-75.

[8] Berberović, E., van Hinsberg, N. P., Jakirlić, S., Roisman, I. V., and Tropea, C., "Drop impact onto a liquid layer of finite thickness: Dynamics of the cavity evolution," *Physical Review E*, 79(3), 2009, pp. 036306.

[9] Bai, W., and Taylor, R. E., "Numerical simulation of fully nonlinear regular and focused wave diffraction around a vertical cylinder using domain decomposition," *Applied Ocean Research*, 29(1), 2007, pp. 55-71.

[10] Taylor, R. E., Wu, G., Bai, W., and Hu, Z., "Numerical wave tanks based on finite element and boundary element modeling," *Journal of Offshore Mechanics and Arctic Engineering*, 130(3), 2008, pp. 031001.

[11] Bai, W., and Taylor, R. E., "Fully nonlinear simulation of wave interaction with fixed and floating flared structures," *Ocean engineering*, 36(3), 2009, pp. 223-236.

[12] Bai, W., Feng, X., Taylor, R. E., and Ang, K., "Fully nonlinear analysis of near-trapping phenomenon around an array of cylinders," *Applied Ocean Research*, 44, 2014, pp. 71-81.

[13] Bingham, H. B., and Zhang, H., "On the accuracy of finite-difference solutions for nonlinear water waves," *Journal of Engineering Mathematics*, 58(1-4), 2007, pp. 211-228.

[14] Engsig-Karup, A. P., Bingham, H. B., and Lindberg, O., "An efficient flexible-order model for 3D nonlinear water waves," *Journal of computational physics*, 228(6), 2009, pp. 2100-2118.

[15] Ma, Q., Wu, G., and Eatock Taylor, R., "Finite element simulation of fully non-linear interaction between vertical cylinders and steep waves. Part 1: methodology and numerical procedure," *International Journal for Numerical Methods in Fluids*, 36(3), 2001, pp. 265-285.

[16] Ma, Q., Wu, G., and Eatock Taylor, R., "Finite element simulations of fully non-linear interaction between vertical cylinders and steep waves. Part 2: numerical results and validation," *International Journal for Numerical Methods in Fluids*, 36(3), 2001, pp. 287-308.

[17] Zhou, B., Ning, D., Teng, B., and Bai, W., "Numerical investigation of wave radiation by a vertical cylinder using a fully nonlinear HOBEM," *Ocean Engineering*, 70, 2013, pp. 1-13.

[18] Ning, D.-Z., Shi, J., Zou, Q.-P., and Teng, B., "Investigation of hydrodynamic performance of an OWC (oscillating water column) wave energy device using a fully nonlinear HOBEM (higher-order boundary element method)," *Energy*, 83, 2015, pp. 177-188.

[19] Mehmood, A., Graham, D. I., Langfeld, K., and Greaves, D. M., "Numerical Simulation of Nonlinear Water Waves based on Fully Nonlinear Potential Flow Theory in OpenFOAM®-Extend," *Proc. The 26th International Ocean and Polar Engineering Conference*, International Society of Offshore and Polar Engineers.

[20] Mayer, S., Garapon, A., and Sørensen, L. S., "A fractional step method for unsteady free surface flow with applications to nonlinear wave dynamics," *International Journal for Numerical Methods in Fluids*, 28(2), 1998, pp. 293-315.

[21] Wu, G., Ma, Q., and Taylor, R. E., "Numerical simulation of sloshing waves in a 3D tank based on a finite element method," *Applied ocean research*, 20(6), 1998, pp. 337-355.

[22] Shao, Y.-L., and Faltinsen, O. M., "A harmonic polynomial cell (HPC) method for 3D Laplace equation with application in marine hydrodynamics," *Journal of Computational Physics*, 274, 2014, pp. 312-332.

[23] Lin, P., and Li, C., "A σ-coordinate three-dimensional numerical model for surface wave propagation," *International Journal for Numerical Methods in Fluids*, 38(11), 2002, pp. 1045-1068.

[24] Bai, W., Mingham, C. G., Causon, D. M., and Qian, L., "Finite volume simulation of viscous free surface waves using

the Cartesian cut cell approach," *International Journal for Numerical Methods in Fluids*, 63(1), 2010, pp. 69-95.

[25] Luth, H., Klopman, G., and Kitou, N., "Project 13g: Kinematics of waves breaking partially on an offshore bar: LDV measurements for wave with and without a net offshore current," *Rep. No. H*, 1573, 1994, pp.

[26] Martínez-Ferrer, P. J., Causon, D. M., Qian, L., Mingham, C. G., and Ma, Z., "A multi-region coupling scheme for compressible and incompressible flow solvers for two-phase flow in a numerical wave tank," *Computers & Fluids*, 125, 2016, pp. 116-129.

[27] Martínez-Ferrer, P. J., Qian, L., Ma, Z., Causon, D. M., and Mingham, C. G., "Improved numerical wave generation for modelling ocean and coastal engineering problems," *Ocean Engineering*, 152, 2018, pp. 257-272.